View metadata, citation and similar papers at core.ac.uk

brought to you by CORE

provided by Elsevier - Publisher Connector

FEBS Letters 588 (2014) 3603–3612

journal homepage: www.FEBSLetters.org

Review

Twinkle, twinkle little star: Photoswitchable fluorophores for super-resolution imaging

Tyler J. Chozinski [a,1], Lauren A. Gagnon [a,1], Joshua C. Vaughan [a,b,*]

[a] Department of Chemistry, University of Washington, Seattle, WA, USA
[b] Department of Physiology and Biophysics, University of Washington, Seattle, WA, USA

ARTICLE INFO

Article history:
Received 1 May 2014
Revised 14 June 2014
Accepted 16 June 2014
Available online 7 July 2014

Edited by Elias M. Puchner, Bo Huang, Hermann E. Gaub and Wilhelm Just

Keywords:
Super-resolution imaging
Fluorophore
Photoswitch

ABSTRACT

Photoswitchable fluorescent probes are key elements of newly developed super-resolution fluorescence microscopy techniques that enable far-field interrogation of biological systems with a resolution of 50 nm or better. In contrast to most conventional fluorescence imaging techniques, the performance achievable by most super-resolution techniques is critically impacted by the photoswitching properties of the fluorophores. Here we review photoswitchable fluorophores for super-resolution imaging with discussion of the fundamental principles involved, a focus on practical implementation with available tools, and an outlook on future directions.
© 2014 Federation of European Biochemical Societies. Published by Elsevier B.V. All rights reserved.

1. Introduction

Fluorescence microscopy allows researchers to explore the inner workings of fixed or living specimens in order to directly monitor organization and dynamics occurring within a given microenvironment. Its immense popularity arises in large part from the ability to specifically label molecules or structures of interest within a cell and from its ability to study living organisms. While fluorescence microscopy has revolutionized the visualization of structures and dynamics in biology, it has traditionally faced a resolution limit of about 250 nm laterally and 500 nm axially, such that features closer than these distances are obscured. This resolution limit is caused by the diffraction of light and is a characteristic of all far-field light microscopies, where far-field here refers to configurations where a detector is placed several wavelengths or further from the emitting dipole. Other biological imaging modalities such as electron microscopy, atomic force microscopy, or near-field techniques that place a detector or imaging probe within approximately one wavelength or less of the emitting dipole, are capable of attaining very high spatial resolution but either have a poor ability to identify the molecules being examined or are primarily limited to the imaging of surface features.

Recently, however, super-resolution fluorescence imaging techniques have emerged which are able to achieve a resolution of ~50 nm or better while maintaining the high molecular specificity and live-cell compatibility of conventional fluorescence microscopy [1,2]. These advances rely critically upon the ability to manipulate fluorophores between bright and dark states in order to reveal sub-diffraction limit spatial information about samples being studied. In this review we will focus on photoswitchable fluorophores for super-resolution fluorescence microscopy, including a discussion of how they impact imaging performance, recent developments in the field, and ongoing areas where additional work is needed. There are already many excellent reviews on super-resolution microscopy techniques and we refer the reader to these for more detailed discussion of the techniques [1–7].

Far-field super-resolution methods fall loosely into two categories. Techniques such as stimulated emission depletion (STED) microscopy, the related technique reversible saturable optically linear fluorescence transitions (RESOLFT) microscopy, and saturated or photoswitching structured illumination microscopy

Abbreviations: STED, stimulated emission depletion; RESOLFT, reversible saturable optically linear fluorescence transitions; SIM, structured illumination microscopy; STORM, stochastic optical reconstruction microscopy; PALM, photoactivated localization microscopy; FPALM, fluorescence PALM; psSIM, photoswitching SIM; TCEP, tris 2-carboxyethylphosphine; SOFI, super-resolution optical fluctuation imaging; PAINT, points accumulation by imaging in nanoscale topography

* Corresponding author. Address: Department of Chemistry, Box 351700, University of Washington, Seattle, WA 98195, USA. Fax: +1 206 685 8665.
E-mail address: jcv2@uw.edu (J.C. Vaughan).

[1] These authors contributed equally to this work.

http://dx.doi.org/10.1016/j.febslet.2014.06.043
0014-5793/© 2014 Federation of European Biochemical Societies. Published by Elsevier B.V. All rights reserved.

(SIM) use patterned illumination in combination with saturation effects to generate signal from only a subset of molecules within a diffraction-limited region (see Fig. 1) [8–11]. In the case of STED, a donut-shaped depletion beam of wavelength longer than the detected fluorescence band is typically used to stimulate emission of light from excited state molecules at the periphery of a diffraction limited spot. When stimulated emission is driven to a saturating regime, only excited state fluorophores at the center of the donut (which has approximately zero intensity) are able to emit fluorescence. The approach is generalized in the technique RESOLFT, which can use transitions other than stimulated emission to reduce the volume from which signal is emitted. In RESOLFT this is often done by using a donut-shaped beam to photoswitch the molecules at the periphery of a diffraction-limited spot to a long-lived dark state, achieving a similar result as with STED where fluorescence is only detected from molecules at the center of the donut. The experiment for STED or RESOLFT may then be scanned and repeated over the entire region of interest to create a super-resolution image. Linear SIM [12] is an elegant technique capable of an approximately twofold resolution improvement over conventional fluorescence microscopy, and when extended to non-linear regimes through saturated excitation [10] or saturated photoswitching [11], can in principle achieve diffraction-unlimited resolution as for STED and RESOLFT.

A second category of super-resolution imaging uses sequential localization of individual fluorescent probes to build up a high resolution image of the fluorophores labeling the sample (see Fig. 1).

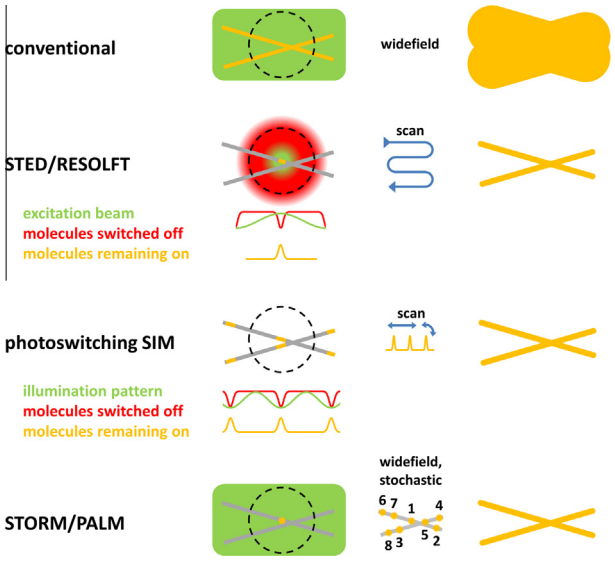

Fig. 1. Schematics for conventional and super-resolution fluorescence microscopy. In conventional imaging, a small object consisting of two crossed lines produces a blurry image (top right) due to the diffraction of light. The dashed circle indicates the ~250 nm size of a diffraction limited spot which characterizes the resolution of conventional fluorescence microscopy. In STED and RESOLFT, the molecules at the periphery of the diffraction limited spot are switched off using a donut-shaped beam with saturated illumination, such that only fluorophores in the middle of the donut are visualized. Molecules are switched back on (for RESOLFT) and then the procedure is repeated and raster scanned across the sample to record a super-resolution image. In photoswitching SIM (psSIM), a saturating sinusoidal illumination pattern (green) is used to switch off all molecules except those near the minima (zeros) of the pattern. The molecules remaining on are imaged by phase shifting the sinusoidal illumination pattern by half a cycle and then the molecules are switched back on with illumination at a new wavelength. The sinusoidal pattern is then scanned over the sample at different phases and angles, and the full image series is analyzed to extract a super-resolution image. In STORM/PALM, individual fluorophores (numbered 1–8) are sequentially activated, imaged, and bleached using widefield illumination, and a super-resolution image is reconstructed from fitted positions of the individual fluorophores.

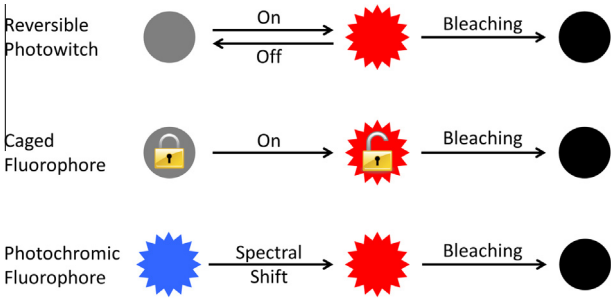

Fig. 2. Overview of different types of photoswitching used in super-resolution fluorescence microscopy. Gray circles indicate non-emissive fluorophores, while black circles indicate bleached fluorophores. Red and blue stars indicate fluorophores emitting red or blue light.

This is typically achieved by initially switching off the fluorescence from the fluorophores labeling the sample and subsequently activating a sparse subset of molecules to a fluorescent state. The subset of activated molecules is sufficiently sparse that one or fewer molecules is activated at any point in time within a diffraction-limited region. These activated molecules are imaged onto a sensitive camera or detector, switched off or bleached, and the process is repeated many times until all or a sufficient number of fluorophores have been recorded. The images of the activated fluorophores are individually analyzed to determine their positions with low uncertainty [13,14], and a final image is reconstructed from the determined positions of the fluorophores. The technique is known as stochastic optical reconstruction microscopy (STORM) [15], photoactivated localization microscopy (PALM) [16], fluorescence PALM (FPALM) [17], and numerous subsequent acronyms, but all share the same basic single-fluorophore approach. For brevity, we will refer to this family of techniques simply as STORM/PALM.

Despite substantial differences in implementation, these far-field super-resolution techniques share several common features. Fundamentally, they all use some sort of switching mechanism to reduce the volume of the emitting signal, where the single molecule approach may perhaps be seen as limit of the smallest possible emitting volume. The reduction of the emitting volume is achieved in most super-resolution techniques by photoswitching fluorophores between long-lived bright and dark states, and this is used for STORM, psSIM, and most implementations of RESOLFT. As such, there are special requirements on the fluorophores used in these methods which have not previously been important for conventional fluorescence microscopy techniques. It is important to note that STED does not switch off fluorescence by means of long-lived dark states, but does use light to suppress signal for most excitation events, and that this also places specific demands on fluorophores. Fig. 2 provides an overview of the different types of photoswitching used in super-resolution fluorescence microscopy.

2. Properties of fluorescent probes for super-resolution imaging

Photoswitchable fluorophores are relative newcomers to bioimaging; however, they have made appearances in the literature well before the advent of super-resolution imaging. For example, Mitchison created a photoactivatable fluorescein derivative covalently linked to tubulin and subsequently used this to observe microtubule polymerization at kinetochores [18,19]. Although photoswitches are becoming more popular among the biological imaging community, photoswitches have been known for decades for non-bioimaging applications (e.g., diarylethenes, spiropyrans, etc.) [20,21]. Several key parameters describe the photoswitching

behavior, including on–off contrast ratio, number of switching cycles, duty cycle, photons per switching event, switching cycle rate, dependence of these properties on illumination intensity and chemical environment. These parameters are in addition to general fluorophore properties to consider, including extinction coefficient, quantum yield, absorption and fluorescence wavelengths, photostability, and water solubility, etc.

The *on–off contrast* is the brightness of the fluorophore in the 'on' state divided by that of the 'off' state. This property impacts the ability to generate contrast between the fluorophores in the reduced volume of a diffraction-limited region compared to that of the remainder of the fluorophores in the diffraction limited region. If the on–off contrast ratio is low (poor), then it is difficult to detect fluorescence from a small sub-region of a diffraction-limited spot since the fluorophores outside of that sub-region would provide a large competing signal that effectively blurs out the measurement. For this reason, a high on–off ratio is generally desired. The analogue in STED is determined by efficiency of the donut-shaped depletion beam in suppressing fluorescence from the excited state fluorophores.

Photoswitchable fluorophores typically transit between bright and dark states some number of times before irreversibly photobleaching. The *number of switching cycles* achievable with a given fluorophore and/or condition imposes limitations depending on the imaging modality. For techniques like RESOLFT or psSIM, the fluorophores in a given diffraction limited region must be photoswitched many times in order to record a single super-resolution image. The analysis routines used in these techniques also typically assume that there is little photobleaching during the acquisition of a set of data to generate one super-resolution image, so it is desirable to have a photoswitchable molecule which can be switched many times. For STORM/PALM, a single cycle of photoswitching is sufficient, though the use of several switching cycles does improve image resolution by averaging out stochastic localization errors [22]. Fluorophores in STED must also be able to be scanned many times, and premature bleaching may be problematic due to the possibility of the intense STED beam exciting fluorophores to high-lying excited states that are rapidly bleached. Additionally, when imaging dynamics in living specimens or specimens which change over time, many switching cycles are generally desired for all of the super-resolution imaging techniques. On the other hand, for STORM/PALM, a single photoactivation followed by irreversible photobleaching would in principle provide a particularly clean way to report on numbers of dye molecules decorating a sample and, with sufficiently well-characterized labeling strategies, could directly report on analyte stoichiometry. Despite the present lack of a 'perfect' single-cycle photoswitch, however, strategies which account for multiple photoswitching cycles have nonetheless made good progress in determining stoichiometry [23–25].

Two properties of photoswitches are especially important for STORM/PALM, namely photons per switching event and duty cycle. The *number of detected photons* per switching event is typically the main factor dictating the uncertainty of determining a fluorophore's position, where the uncertainty scales roughly as the inverse square root of the number of detected photons [13,26]. In a sense, this uncertainty determines the reduced volume achieved for STORM/PALM compared to the diffraction limited region (Fig. 1), but does not solely determine the achievable resolution, since it does not factor in the achievable density of labels. It is the *duty cycle*, or fraction of time a fluorophore spends in an on state, which limits the maximum density of fluorophores that may be localized in a diffraction-limited region, with approximately an inverse relationship between fluorophore density and duty cycle [22]. This limit on fluorophore density is a simple consequence of the Nyquist sampling theorem, which states that the maximum attainable resolution is equal to twice the average distance between adjacent probes [27]. Together, photons per localization and duty cycle limit the spatial resolution achievable by STORM/PALM.

The on and off *switching rates* limit the speed with which super-resolution images may be recorded and are important factors governing the temporal resolution achievable with super-resolution imaging. Slower photoswitching rates require more acquisition time while faster photoswitching rates accommodate faster data acquisition. In many cases the photoswitching rates are controllable by illumination at one or more wavelengths or by changing the chemical composition of the imaging cocktail (see below).

Additional properties are worth noting, although we will not discuss them in detail here. Illumination of biological specimens with intense visible or ultraviolet light can lead to phototoxicity, in particular when labeled with fluorophores that can produce reactive oxygen species, and it is important for live-cell imaging experiments to assess potential artifacts due to phototoxicity [28]. For STORM/PALM, errors in position determination may occur if fluorophores are not freely rotating on the time scale of the measurements, especially for molecules observed slightly above or below the optimum focus [29–32]. Compatibility with multicolor imaging is another key property. For example, some popular STORM/PALM fluorophores, such as EosFP and its relatives, initially fluoresce in the green region of the spectrum (~515 nm) and photoconvert to fluoresce in the orange/red (~575 nm, see also Fig. 2). This means that EosFP consumes two emission channels, leaving less options available for multicolor imaging, and thus motivating the search for fluorophores which maintain all the other desirable qualities but which do not cause spectral interference [27,33].

With all of these important fluorophore properties for super-resolution imaging, it should not be a surprise that there is a large amount of variability in fluorophore performance. Stefan Hell's group has assembled a list of many fluorophores used in STED along with the reported resolution and the conditions used (e.g. depletion wavelength and pulse length) [34]. The attainable resolution varies between 16–140 nm, and perhaps future efforts will help to provide insights into what properties of the fluorophores lead to better or worse resolution. Recent work has systematically evaluated many organic fluorophores and fluorescent proteins for use in STORM/PALM, and as with STED, some STORM/PALM fluorophores achieved excellent results while others performed poorly or were practically useless [22,35]. This is in stark contrast to conventional fluorescence microscopy, where most fluorophores with good general properties (i.e., high extinction coefficient, quantum yield, and photostability) work very well.

While fluorophore structure strongly impacts photoswitching performance, in many cases, the chemical environment of the fluorophores during imaging (which we refer to as the 'imaging cocktail') also exerts a strong influence on performance. For instance, in the case of the fluorophore Cy5 (which is a close structural relative of AlexaFluor 647, and which we use synonymously with AlexaFluor 647 in this paper) there are at least five substantially different imaging cocktails which have been reported in the literature. The original STORM/PALM publication with Cy5 used an imaging cocktail containing an oxygen scavenger system and thiol to facilitate photoswitching [15]. Subsequently, it has been shown that Cy5 may be: switched on and off using redox chemistry with ascorbic acid [36]; reduced with $NaBH_4$ to a long-lived non-fluorescent form and photoactivated [32]; switched on and off using the phosphine TCEP (tris 2-carboxyethly phosphine) [37]; switched on and off using a thiol and a mixture of either cyclooctatetraene or unknown additives in the proprietary sample mounting medium Vectashield [38,39]. For these different schemes, photons detected per localization varied between ~100–1 000 000, and duty cycle, which is generally harder to measure, in the neighborhood of

10^{-2} to 10^{-6}. On the one hand, the ability to tune the photoswitchable properties of a given fluorophore is incredibly powerful, and yet on the other hand presents a liability if the imaging cocktail is incorrectly formulated.

3. Fluorescent proteins for super-resolution imaging

Moerner and coworkers reported GFP and YFP as the first single molecule photoswitches over a decade before super-resolution microscopy techniques became widespread [40]. In the years since the discovery, significant advances have been taken in discovering or developing new fluorescent protein photoswitches and mutants with characteristics tailored for specific experiments, including super-resolution fluorescence imaging applications. Several recent reviews summarize many of these developments in the context of super-resolution imaging [41–45].

In general, fluorescent proteins have the great advantages of a relatively small size (compared, for instance, to fluorescently labeled antibodies), convenient genetic encodability for tagging proteins or molecules which are bound by proteins, and excellent compatibility with imaging living samples. The photostability or number of photons per switching cycle of fluorescent proteins tends to be lower than that of popular small organic dyes and multicolor super-resolution fluorescence imaging with fluorescent proteins is still challenging. In contrast, the duty cycle of many fluorescent proteins may be 1–3 orders of magnitude better than that of popular organic fluorophores [22,35]. Furthermore, as with any experiments involving tagged proteins, practitioners should be cautious to avoid problems related to overexpression, codon optimization, oligomerization or aggregation, perturbation of sensitive proteins, or endogenous untagged protein that may be unobservable in an experiment [35]. Depending on the experiment, the maturation time and the impact of the tag on expression levels of the fusion protein may also be important considerations [35].

Fluorescent proteins used in super-resolution fluorescence microscopy come in several broad categories. Those used in STED must resist photobleaching while illuminated with the relatively intense excitation and depletion beams. In contrast, the fluorescent proteins used in RESOLFT, psSIM, and STORM/PALM must be photoswitchable in some way. This includes fluorescent proteins which are initially dark and may be photoactivated either irreversibly (such as photoactivatable GFP) or reversibly (such as Dronpa) [47,48]. Other fluorescent proteins, such as EosFP, are instead able to irreversibly convert from a green fluorescent form to a red-fluorescent form, such that when viewed in the red channel, the fluorescent protein appears to photoactivate [49]. While the green to red photoconversion is irreversible, many of these fluorophores also exhibit blinking behavior in the red form which may confuse quantification efforts if not properly handled [50,51]. There are also fluorescent proteins which exhibit a combination of these two behaviors, such as IrisFP which is photoconvertible between green and red fluorescent states and also exhibits reversible photoactivation in both the green and red fluorescent forms [46]. The basic switching behaviors are illustrated in Fig. 3 and a table summarizing photoswitching properties of a number of fluorescent proteins are shown in Table 1.

STED microscopy has utilized many fluorescent proteins in super-resolution imaging to date. GFP, YFP, citrine and others have been used for ~50–70 nm resolution imaging with good results in both fixed and living cells [52–60]. In a particularly impressive demonstration, YFP was used to image dendrites in the brain of a living mouse at <70 nm resolution [61]. Multicolor imaging with STED faces the challenge of accommodating different excitation and depletion wavelengths along with the excitation and emission bands of each fluorophore. One approach to this challenge has been to use common excitation and depletion wavelengths for two fluorophores with nearby emission bands that are separable using spectral unmixing techniques, for instance using the GFP/YFP pair where ~100 nm resolution with ~10% crosstalk was achieved [62].

Numerous reversible photoswitchable fluorophores have been utilized for RESOLFT and photoswitching SIM, including several recent excellent additions to the arsenal. Compared to imaging by STED, these probes can operate at orders of magnitude lower illumination intensities, such that phototoxicity concerns for imaging living samples are greatly reduced. Dronpa has been used for photoswitching SIM, and, under optimized conditions that yielded ~65 switching cycles, has achieved <50 nm resolution of various in vitro or cellular structures [11]. In 2011, Stefan Hell, Stefan

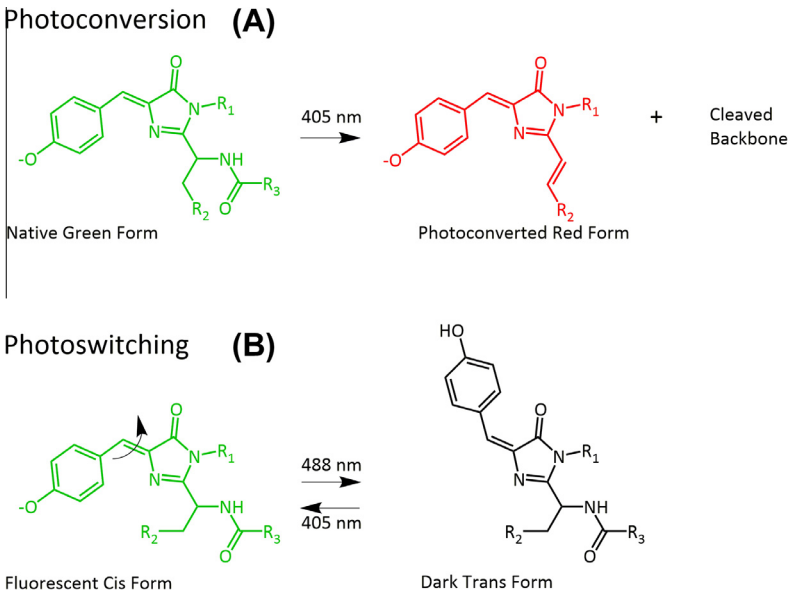

Fig. 3. Representative photoswitching mechanisms of fluorescent proteins. (A) FPs such as EosFP convert irreversibly from a green fluorescent form to a red fluorescent form upon illumination with violet or ultraviolet light. The photochromic shift occurs due to cleavage of the peptide backbone which extends the conjugation of the chromophore and red-shifts the absorption and emission spectra by 50–60 nm. (B) FPs such as Dronpa undergo reversible *cis–trans* isomerization, where the *cis* form is fluorescent and the *trans* form is dark. Other fluorescent proteins may use a combination of these phenomena, such as IrisFP [46].

Table 1
A selection of fluorescent proteins used for super-resolution fluorescence imaging. In the notes field, each fluorescent protein's oligomeric state is indicated (m = monomer, d = dimer, wd = weak dimer, t = tetramer) along with a code for the type of fluorophore (ps = reversibly photoswitchable, pa = photoactivatable, pc = photoconvertible). The properties of the fluorescent forms of these fluorophores used for super-resolution imaging are tabulated here: λ_{ex} (excitation wavelength); λ_{em} (emission wavelength); $\lambda_{on/off}$ (wavelengths for switching the fluorescence on and off, respectively); ε (extinction coefficient); Φ (fluorescence quantum yield); on–off contrast ratio (ratio of intensity of the emissive form to the dark form); *N* (number of switching cycles, including reported blinking events after irreversible photoconversion [51]); phot. (number of detected photons per localization event); ND indicates the parameter was not determined.

Fluorescent proteins used in super-resolution imaging

STED fluorophores	Notes	λ_{ex} (nm)	λ_{em} (nm)	λ_{STED} (nm)	ε (M^{-1} cm^{-1})	Φ	Resolution reported				References
EGFP	m	490	510	575	55000	0.6	~70 nm				[52–55]
EYFP	m	514	527	598	36500	0.63	<100 nm				[52,55,56]
Citrine	m	516	529	592	77000	0.76	<60 nm				[52,57,58]
E2Crimson	t	611	646	760	126000	0.23	<100 nm				[52,59]
TagRFP657	m	611	657	750	34000	0.1	~74 nm				[52,60]
RESOLFT/psSIM fluorophores	**Notes**	**λ_{ex} (nm)**	**λ_{em} (nm)**	**$\lambda_{on/off}$ (nm)**	**ε (M^{-1} cm^{-1})**	**Φ**	**On–off contrast**	***N***			**References**
Dronpa	m, ps	503	518	405/488	95000	0.85	~30	60–70			[11,71,72]
rsEGFP	m, ps	493	510	405/491	47000	0.36	50	>1100			[63,65]
rsEGFP2	m, ps	478	503	430/488	61300	0.3	ND	>2000			[65,66]
Dreiklang	m, ps	511	529	340/412	83000	0.41	75	>160			[43,64]
rsCherryRev1.4	d, ps	572	609	430/592	ND	ND	ND	>1000			[66]
STORM/PALM fluorophores	**Notes**	**λ_{ex} (nm)**	**λ_{em} (nm)**	**$\lambda_{on/off}$ (nm)**	**ε (M^{-1} cm^{-1})**	**Φ**	**On–off contrast**	***N***	**Phot.**	**Duty cycle**	**References**
PAmcherry1	m, pa	564	595	~370 on	18000	0.46	4000	1 (1)	~725	8×10^{-6}	[33,35,51]
Dronpa	m, ps	503	518	405/488	95000	0.85	ND	60–70	120	8×10^{-4}	[11,35,41,71]
Dreiklang	m, ps	511	529	340/412	83000	0.41	75	ND	400–700	ND	[43,64,73]
MEos2	wd, pc	569	581	405/573	41000	0.55	ND	1 (2.8)	~1000	3×10^{-6}	[35,51,67–69]
MEos3.2	m, pc	572	580	405/572	32200	0.55	ND	1 (2.4)	~1000	3×10^{-6}	[35,51,70]
mMaple	wd, pc	566	583	380/566	30000	0.56	ND	1 (3.4)	~1000	2×10^{-6}	[35,51,69]
mMaple2	m, pc	566	583	405/566	ND	ND	ND	ND	~800	1×10^{-6}	[35]

Jakobs, and coworkers reported two newly developed photoswitchable fluorescent proteins, dubbed Dreiklang and reversibly switchable enhanced GFP (rsEGFP), which can photoswitch more than 160 and 1000 cycles, respectively [63,64]. Using these low-fatigue probes, they achieved <40 nm resolution imaging in fixed cells. Subsequently, these proteins and some more recently developed ones such as rsEGFP2, rsCherryRev1.4, and others have found application in one- and two-color RESOLFT imaging in fixed or living cells at 50–100 nm resolution [65,66]. Many of the reversibly photoswitchable fluorescent proteins are switched off using the same wavelength as the imaging wavelength and are switched on with ultraviolet light.

For STORM/PALM, EosFP and many of its close relatives have been popular choices for fluorescent labels owing to their good on–off contrast, duty cycle, and relatively high value number of detected photons per localization (~1000 photons) [67–70]. The original tdEosFP was an obligate tetramer and has been extensively engineered to create variants which have little to no tendency to aggregate but which still maintain the desirable optical properties of the chromophore [49,67,70]. The reversibly photoswitchable fluorescent protein Dreiklang, also described above for RESOLFT (or psSIM, in principle) emits ~400–700 detected photons/localization for many cycles and ~35 nm localization uncertainty, is particularly interesting for live-cell applications where many snapshots would be desired [64]. Other variants include mMaple2 which, like the EosFP variants, emits a good number of photons (~800 detected photons/localization) but shows a superior efficiency of expression/folding/maturation and lacks the tendency to form dimers of the original mMaple variant [35,69]. A major current limitation is that the options for two-color (or more) STORM/PALM using fluorescent proteins are at present quite limited. This limitation arises in part since photoconvertible fluorescent proteins are preferred due to their relatively high photons/localization but also has the consequence that the two main fluorescent protein channels are consumed by a single probe.

4. Organic fluorophores for super-resolution imaging

Intermittent emission from single organic fluorophores was observed in many of the earliest single molecule fluorescence measurements [74,75]. Approximately a decade later, the particularly robust Cy5 photoswitch was reported and then applied to super-resolution imaging by STORM/PALM [15,76,77]. Over the next few years, several groups reported the use of a range of established organic fluorophores for imaging by STORM/PALM, with a fair amount of variability in procedures and performance [78–80]. Meanwhile, STED, which utilizes the universal property of stimulated emission rather than photoswitching to long-lived dark states, had been demonstrated with many organic dyes [52]. RESOLFT/psSIM have been less utilized with organic fluorophores, and we will omit these from our discussion on organic fluorophores except to point out here that low switching intensity organic fluorophores with a large number of switching cycles would be particularly helpful for these techniques.

In general, the best organic fluorophores are substantially brighter and more resistant to bleaching than their best fluorescent protein counterparts and also have the advantage of small size. For instance, the dye Abberior STAR 635P can achieve a resolution in STED which is approximately two times better than the best resolution achievable with any of the fluorescent proteins, presumably due to a high photostability [81,82], and in STORM/PALM, the dye Cy5 gives several times more photons per localization than any of the currently preferred photoswitchable fluorescent proteins [22,68–70]. Because there are a wide array of organic fluorophores spanning the visible and near infrared region of the electromagnetic spectrum, there are many good options for multicolor imaging of cellular structures for both STED and STORM/PALM [22,78,81,83,84]. Notably, the duty cycle of many photoswitchable fluorescent proteins is 10–1000 times lower than many of the currently favored photoswitchable organic fluorophores, and may enable experiments at higher densities with photoswitchable

fluorescent proteins than is achievable with photoswitchable organic fluorophores [22,35].

Organic fluorophores are not without their drawbacks, however, and in many cases have inferior properties for labeling samples compared to fluorescent proteins. The use of indirect or direct immunofluorescence with bulky dye-conjugated antibodies may blur out structures of interest and in most cases requires fixation and permeabilization of the specimen to accommodate staining. The advent of small, single-chain antibodies raises the prospect of using small epitope tags with minimal blurring effects [85], although these are at present only commercially available for targeting a very small number of proteins or epitope tags and in any event are primarily restricted to use in non-living specimens. Some organic fluorophores are able to label specific cellular structures of interest in live or fixed specimens by virtue of the intrinsic properties of the fluorophore or an attached moiety [86,87], but the approach is limited to fairly a small subset of organelles or structures (e.g. mitochondria, the plasma membrane, cytoskeleton, etc.). A growing body of labeling techniques utilizes reactive protein tags that can recognize a fluorophore conjugated to a substrate which may be bound by or covalently linked to the reactive protein [88–90]. While these reactive labeling techniques offer the prospects of the best of both worlds, at present, many of the desirable organic fluorophores are not cell-permeant and thus practitioners may be restricted to the use of cell-permeant fluorophores or the use of dye delivery of impermeant fluorophores by bead loading, pinocytosis, or electroporation [68].

Organic fluorophores photoswitch by a variety of mechanisms. For instance, Cy5 has been shown to react with thiols upon illumination with red light, or with the phosphine TCEP (tris 2-carboxyethylphosphine) in the absence of light, to generate a non-fluorescent adduct [37,91]. The adduct consists of the addition of the thiol or phosphine to the polymethine bridge of Cy5 such that the conjugation of dye is disrupted and the molecule's absorption shifts to the ultraviolet (Fig. 4). In contrast, several rhodamine fluorophores have been shown to generate long-lived non-fluorescent radical species which can also be photoactivated by illumination with ultraviolet light [92]. Yet a third mechanism for photoswitching has been established for the oxazine dye Atto 655, which undergoes two one-electron reactions to generate a reduced form of the dye and which is also activatable by illumination with ultraviolet light [92,93]. Some fluorophores are prepared chemically in a dark form and may be photoactivated by illumination with, for instance, ultraviolet light [32,94–98]. The details of many of these chemical or photochemical reactions require further study. These photoswitching properties have been primarily utilized for STORM/PALM, to date. As mentioned earlier, in STED, it is stimulated emission of molecules at the periphery of a diffraction limited region which leads to reduction of the imaging volume. While stimulated emission is a process common to all fluorophores, transitions to higher lying states that can lead to premature photobleaching tends to be one of the key factors that renders a fluorophore unsuitable for STED.

STED has been used with a wide range of organic fluorophores and many recent developments have in particular improved the technique's multicolor capabilities. These include long-established STED fluorophores such as Chromeo 488, Atto 565, and Atto 647 N, as well the recent rhodamine derivatives, carbopyronine derivatives, or Abberior STAR series fluorophores which are now commercially available (e.g., Abberior STAR 635P) [34,52,81,82,99,100]. Multicolor imaging strategies include the use of common excitation and depletion wavelengths with closely emitting fluorophores (e.g., that can be separated through spectral unmixing techniques, as was described above for two-color fluorescent protein imaging). A second strategy utilizes two fluorophores with well-separated excitation and emission spectra (e.g., Atto 590 and Abberior STAR 635P) whose fluorescence emission can be switched off with a common depletion beam [101]. The use of a common depletion beam in both of these approaches helps to ensure good channel registration and also helps minimize complexity and cost in the apparatus.

A wide range of organic fluorophores have also been employed in STORM/PALM, including representatives from many popular general classes of fluorophores such as rhodamines, cyanines, oxazines, carbopyronines, bodipy fluorophores and others [22,78–80,86,98,102]. The results obtainable with the fluorophores vary widely, however, and as with STED fluorophores, it is recommended to choose STORM/PALM fluorophores carefully. A recent systematic comparison of many commercially available organic fluorophores for STORM/PALM [22] established good metrics for evaluating fluorophore fitness and identified several very good fluorophores amongst the panel and conditions tested. One key finding of interest to practitioners is that when using the popular oxygen scavenger/thiol based imaging cocktail, the best results amongst the explored dyes and conditions were obtained with Cy5 (or AlexaFluor 647) and the best four-color results were obtained with Atto 488/Cy3B/AlexaFluor 647/DyLight 750. Subsequent reports from the same group include an improved two-color imaging scheme based on phosphine quenching of cyanine fluorophores [37], organelle/membrane probes for live-cell STORM/PALM imaging [86], and reductively caged fluorophores which when activated in an optimized imaging cocktail [103,104] can yield 10–1000 times greater photons per localization [32]. Data for a subset of these fluorophores are summarized in Table 2.

Beyond utilizing long-established, commercially available fluorophores, there has been growing interest in the development of new fluorophores or fluorophore variants that are tuned for one or more super-resolution methods, including STORM/PALM.

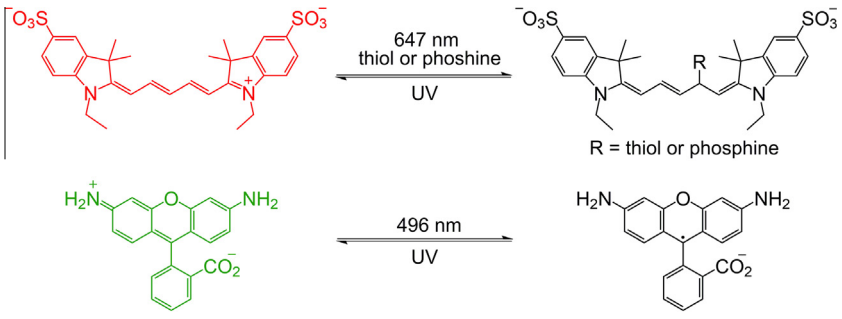

Fig. 4. Example mechanisms for photoswitching of a cyanine and rhodamine fluorophore. (Top) Upon incubation with a phosphine or illumination with 647 nm light in the presence of a thiol or phosphine, Cy5 transitions to a non-fluorescent state adduct consisting of the phosphine or thiol bound to the polymethine bridge. Illumination with ultraviolet light can dissociate the adduct. (Bottom) Several rhodamine fluorophores can be converted to a long-lived, non-fluorescent radical upon illumination with light at their main absorption band in the absence of oxygen. The dark form may be photoactivated by illumination with ultraviolet light.

Table 2
A selection of small organic fluorophores used for super-resolution fluorescence imaging. In the notes field for STORM/PALM fluorophores, a two letter code for the type of fluorophore is indicated in each case (ps = reversibly photoswitchable, pa = photoactivatable). For photoswitched fluorophores in the STORM/PALM section, the use of a thiol or phosphine switching agent is indicated by (thiol) or (TCEP, for tris 2-carboxyethylphosphine), while photoactivated/caged fluorophores lack the designation. The properties of the fluorescent forms of these fluorophores used for super-resolution imaging are tabulated here: λ_{ex} (excitation wavelength); λ_{em} (emission wavelength); $\lambda_{on/off}$ (wavelengths for switching the fluorescence on and off, respectively); ε (extinction coefficient); Φ (fluorescence quantum yield); duty cycle (fraction of time spent in the on state); N (number of switching cycles, including reported blinking events after irreversible photoconversion [51]); phot. (number of detected photons per localization event); ND indicates the parameter was not determined. In most cases, on–off contrast values were not reported. Comparably few reports have been published for RESOLFT/psSIM and this section has not been tabulated here.

Organic fluorophores used in super-resolution imaging

STED fluorophore	Notes	λ_{ex} (nm)	λ_{em} (nm)	λ_{STED} (nm)	ε (M^{-1} cm^{-1})	Φ	Resolution reported			References
Chromeo 488		488	517	592	73 000	0.38	30 nm			[52,83,111]
Chromeo 494		494	628	760	55 000	0.28	~80 nm			[52,111,112]
Atto 565		563	592	~662	120 000	0.9	30–60 nm			[52,114,115]
Atto 647N		644	669	~765	150 000	0.5	30–60 nm			[52,83,113–115]
Fl-Rhodamine		633	653	~762	75 000	0.92	~40 nm			[81,82,100,116]
Si-Rhodamine		645	662	~775	100 000	0.39	~50 nm			[117]
AbberiorSTAR635P		635	655	~775	75 000	0.92	~20 nm			[81,82]
STORM/PALM fluorophore	**Notes**	**λ_{ex} (nm)**	**λ_{em} (nm)**	**$\lambda_{on/off}$ (nm)**	**ε (M^{-1} cm^{-1})**	**Φ**	**Duty cycle**	***N***	**Phot.**	**References**
Atto 488 (thiol)	ps	501	523	405/488	90 000	0.8	0.0022	49	1100	[22,115]
Atto 488	pa	501	523	405/488	90 000	0.8	0.002	~1	$\sim10^4$	[22,32,115]
Cy3B (thiol)	ps	559	570	405/561	130 000	0.67	0.0004	5	2050	[22,118]
Cy3B	pa	559	570	405/561	130 000	0.67	0.0004	~1	$\sim10^5$	[22,32,118]
Alexa 647 (thiol)	ps	650	665	405/647	239 000	0.33	0.0007	26	5200	[22,119]
Cy7 (thiol)	ps	747	776	405/750	250 000	0.28	0.0004	~3	1000	[22,118]
Alexa 750 (TCEP)	ps	749	775	405/750	240 000	0.12	0.0004	ND	2800	[22,37,119]
Si-Rhod. (thiol)	ps	645	662	ND/640	100 000	0.39	ND	ND	630	[117]

Amongst these fluorophores are various caged rhodamine or fluorescein derivatives [96–98,105] and fluorophores based on DCDHF (2-dicyanomethylene-3-cyano-2,5-dihydrofuran) [106]. As super-resolution imaging techniques become more widespread and demand grows for excellent super-resolution probes, hopefully these and other optimized compounds become commercially available in order to have broad impact in the hands of researchers.

In contrast to fluorescent proteins, which are typically insensitive to the composition of the imaging solution, organic fluorophores are very sensitive, both in terms of general fluorescence properties (e.g., photostability) and in terms of photoswitching properties. The use of various additives to form an 'imaging cocktail' is an important part of many of these techniques, but often the effects are difficult to interpret since the additives may function in multiple ways. For example, thiols are often added to imaging cocktails and may function as a: triplet state quencher [107]; ligand that forms a non-fluorescent adduct with a dye [91]; reductant which can produce a long-lived, non-fluorescent radical species [92]; deoxygenation agent by reacting with oxygen to form disulfides and water [108]; or perhaps a mixture of these or other yet unidentified roles. The introduction of an oxygen scavenging system can lower oxygen concentrations substantially, but can lead to different outcomes. Oxygen is also a very efficient triplet state quencher which can yield higher fluorescence turnover rates (e.g., more photons per unit time) but which also leads to increased rates of photobleaching. For this reason, single molecule fluorescence studies often utilize an oxygen scavenger system in the imaging cocktail. Use of a reducing and oxidizing system (ROXS), such as the combination of methyl viologen and ascorbic acid together with an oxygen scavenging system, is a popular formulation to minimize photobleaching rates and blinking, although there are exceptions in which fluorophores still show substantial blinking under these conditions [37,104]. Even the use of heavy water (D_2O) can impact photoswitching performance, such as for some oxazine and cyanine dyes which were recently reported to have a higher fluorescence quantum yield and/or higher photons per localization in heavy water as compared to normal water [109,110].

5. Additional super-resolution techniques and fluorescent probes

In this article we have focused on fluorescent proteins and small organic fluorophores used in STED, RESOLFT/psSIM, or STORM/PALM. However, not all established techniques and not all fluorescent probes fit neatly into these categories. For instance, SOFI (super-resolution optical fluctuation imaging) uses higher order statistical analysis of fluctuating fluorescent signals in an image to generate super-resolution fluorescence images even without requiring the localization of individual fluorescent spots [120]. Another technique, dubbed Bayesian localization microscopy, uses a more computation-intensive approach to model an entire set of fluorophore positions in a sample based on a series of measurements during which the fluorophore labels may blink or bleach [121]. Additional classes of fluorescent probes have also been used in super-resolution microscopy, including quantum dots, fluorophores which reversibly bind to a target of interest, and organic fluorophores which turn on as a result of binding.

Quantum dots are intriguing fluorophores due to their high total photon yield and have been used in a number of super-resolution imaging papers. These go back to Lidke et al., whose work on independent component analysis with quantum dots presaged STORM/PALM type localization-based microscopy [122]. Subsequent efforts have found application of quantum dots to imaging by RESOLFT, STORM/PALM, and SOFI although they have not found as frequent use as fluorescent proteins or organic fluorophroes [120,123,124]. One concern regarding the use of core–shell quantum dots (which are also surface-passivated and functionalized) is their relatively large hydrodynamic radius (~20 nm), although this may potentially be improved by the use of smaller quantum dots in the future [125].

A subset of probes used for localization-based microscopy does not utilize photoactivation at all, but instead uses reversible binding with or without a chemical turn-on feature. For instance, Sharonov and Hochstrasser utilized the turn-on fluorescence property of the dye Nile red binding to the plasma membrane in their super-resolution method known as PAINT (points accumulation

by imaging in nanoscale topography) [126]. The approach has since been adapted to use the highly tunable binding/unbinding of fluorescently labeled DNA oligonucleotides to structures labeled with a complementary oligonucleotide, known as DNA-PAINT [127,128]. DNA-PAINT has several attractive aspects, including being compatible with virtually any fluorophore, and the technique will likely find increased usage in coming years.

6. Conclusions

Over the past 5–10 years, super-resolution fluorescence microscopy has evolved from a small number of techniques used by a handful of specialist labs to a wide range of super-resolution techniques which can be found now at many major research institutions around the world. Much of the excitement over these tools relates to the ability to gain sharper glimpses of biological objects whose intrinsic size scales and density are often smaller than the diffraction limit of light, and an untold number of discoveries are hidden just beneath the diffraction limit. At this point in the field, even as the techniques push forward to new frontiers of spatial or temporal resolution or live cell capability, etc., it is more important than ever that new fluorophore developments include adequate characterization of the properties of the fluorophores so practitioners may evaluate whether or not the fluorophore is likely to be useful for their intended application. Hopefully, as super-resolution fluorescence microscopy matures into a workhorse tool for the biological imaging community, this will become standard practice for new reports on fluorophores or fluorophore properties. Only by these efforts can the best tools be placed into the hands of practitioners for widest impact.

Acknowledgements

This work was supported in part by the University of Washington and by a Burroughs-Wellcome Career Award at the Scientific Interface. The authors thank Dr. Aaron R. Halpern (University of Washington) for critical reading of this manuscript.

References

[1] Huang, B., Babcock, H. and Zhuang, X. (2010) Breaking the diffraction barrier: super-resolution imaging of cells. Cell 143 (7), 1047–1058.
[2] Hell, S.W. (2007) Far-field optical nanoscopy. Science 316 (5828), 1153.
[3] Hell, S.W. (2009) Microscopy and its focal switch. Nat. Methods 6 (1), 24–32.
[4] Lippincott-Schwartz, J. and Manley, S. (2009) Putting super-resolution fluorescence microscopy to work. Nat. Methods 6 (1), 21–23.
[5] Heilemann, M. (2010) Fluorescence microscopy beyond the diffraction limit. J. Biotechnol. 149 (4), 243–251.
[6] Schermelleh, L., Heintzmann, R. and Leonhardt, H. (2010) A guide to super-resolution fluorescence microscopy. J. Cell Biol. 190 (2), 165.
[7] Sauer, M. (2013) Localization microscopy coming of age: from concepts to biological impact. J. Cell Sci. 126 (16), 3505–3513.
[8] Klar, T.A. and Hell, S.W. (1999) Subdiffraction resolution in far-field fluorescence microscopy. Opt. Lett. 24 (14), 954–956.
[9] Hofmann, M., Eggeling, C., Jakobs, S. and Hell, S.W. (2005) Breaking the diffraction barrier in fluorescence microscopy at low light intensities by using reversibly photoswitchable proteins. Proc. Natl. Acad. Sci. USA 102 (49), 17565–17569.
[10] Gustafsson, M.G.L. (2005) Nonlinear structured-illumination microscopy: wide-field fluorescence imaging with theoretically unlimited resolution. Proc. Natl. Acad. Sci. USA 102 (37), 13081.
[11] Rego, E.H., Shao, L., Macklin, J.J., Winoto, L., Johansson, G.A., Kamps-Hughes, N., et al. (2012) Nonlinear structured-illumination microscopy with a photoswitchable protein reveals cellular structures at 50-nm resolution. Proc. Natl. Acad. Sci. 109 (3), E135–E143.
[12] Gustafsson, M.G. (2000) Surpassing the lateral resolution limit by a factor of two using structured illumination microscopy. J. Microsc. 198 (2), 82–87.
[13] Thompson, R.E., Larson, D.R. and Webb, W.W. (2002) Precise nanometer localization analysis for individual fluorescent probes. Biophys. J. 82 (5), 2775–2783.
[14] Yildiz, A. and Myosin, V. (2003) Walks hand-over-hand: single fluorophore imaging with 1.5-nm localization. Science 300 (5628), 2061–2065.
[15] Rust, M.J., Bates, M. and Zhuang, X. (2006) Sub-diffraction-limit imaging by stochastic optical reconstruction microscopy (STORM). Nat. Methods 3 (10), 793–796.
[16] Betzig, E., Patterson, G.H., Sougrat, R., Lindwasser, O.W., Olenych, S., Bonifacino, J.S., et al. (2006) Imaging intracellular fluorescent proteins at nanometer resolution. Science 313 (5793), 1642.
[17] Hess, S.T., Girirajan, T.P.K. and Mason, M.D. (2006) Ultra-high resolution imaging by fluorescence photoactivation localization microscopy. Biophys. J. 91 (11), 4258–4272.
[18] Mitchison, T.J. (1989) Polewards microtubule flux in the mitotic spindle: evidence from photoactivation of fluorescence. J. Cell Biol. 109 (2), 637–652.
[19] Sawin, K.E. and Mitchison, T.J. (1991) Poleward microtubule flux mitotic spindles assembled in vitro. J. Cell Biol. 112 (5), 941–954.
[20] Irie, M. (2000) Diarylethenes for memories and switches. Chem. Rev. 100 (5), 1685–1716.
[21] Berkovic, G., Krongauz, V. and Weiss, V. (2000) Spiropyrans and spirooxazines for memories and switches. Chem. Rev. 100 (5), 1741–1754.
[22] Dempsey, G.T., Vaughan, J.C., Chen, K.H., Bates, M. and Zhuang, X. (2011) Evaluation of fluorophores for optimal performance in localization-based super-resolution imaging. Nat. Methods 8 (12), 1027–1036.
[23] Annibale, P., Vanni, S., Scarselli, M., Rothlisberger, U. and Radenovic, A. (2011) Quantitative photo activated localization microscopy: unraveling the effects of photoblinking. PLoS ONE 6 (7), e22678.
[24] Lee, S.-H., Shin, J.Y., Lee, A. and Bustamante, C. (2012) Counting single photoactivatable fluorescent molecules by photoactivated localization microscopy (PALM). Proc. Natl. Acad. Sci. 109 (43), 17436–17441.
[25] Puchner, E.M., Walter, J.M., Kasper, R., Huang, B. and Lim, W.A. (2013) Counting molecules in single organelles with superresolution microscopy allows tracking of the endosome maturation trajectory. Proc. Natl. Acad. Sci. 110 (40), 16015–16020.
[26] Mortensen, K.I., Churchman, L.S., Spudich, J.A. and Flyvbjerg, H. (2010) Optimized localization analysis for single-molecule tracking and super-resolution microscopy. Nat. Methods 7 (5), 377–381.
[27] Shroff, H., Galbraith, C.G., Galbraith, J.A. and Betzig, E. (2008) Live-cell photoactivated localization microscopy of nanoscale adhesion dynamics. Nat. Methods 5 (5), 417–423.
[28] Carlton, P.M., Boulanger, J., Kervrann, C., Sibarita, J.-B., Salamero, J., Gordon-Messer, S., et al. (2010) Fast live simultaneous multiwavelength four-dimensional optical microscopy. Proc. Natl. Acad. Sci. 107 (37), 16016–16022.
[29] Bartko, A.P. and Dickson, R.M. (1999) Imaging three-dimensional single molecule orientations. J. Phys. Chem. B 103 (51), 11237–11241.
[30] Enderlein, J., Toprak, E. and Selvin, P.R. (2006) Polarization effect on position accuracy of fluorophore localization. Opt. Express 14 (18), 8111–8120.
[31] Engelhardt, J., Keller, J., Hoyer, P., Reuss, M., Staudt, T. and Hell, S.W. (2010) Molecular orientation affects localization accuracy in superresolution far-field fluorescence microscopy. Nano Lett. 11 (1), 209–213.
[32] Vaughan, J.C., Jia, S. and Zhuang, X. (2012) Ultrabright photoactivatable fluorophores created by reductive caging. Nat. Methods 28 (9), 1181–1184.
[33] Subach, F.V., Patterson, G.H., Renz, M., Lippincott-Schwartz, J. and Verkhusha, V.V. (2010) Bright monomeric photoactivatable red fluorescent protein for two-color super-resolution sptPALM of live cells. J. Am. Chem. Soc. 132 (18), 6481–6491.
[34] List of dyes used in STED microscopy, <http://nanobiophotonics.mpibpc.mpg.de/old/dyes/>.
[35] S. Wang, J.R. Moffitt, G.T. Dempsey, X.S. Xie, X. Zhuang, Characterization and development of photoactivatable fluorescent proteins for single-molecule-based superresolution imaging, Proc. Natl. Acad. Sci. 2014 (advanced online publication).
[36] Steinhauer, C., Forthmann, C., Vogelsang, J. and Tinnefeld, P. (2008) Superresolution microscopy on the basis of engineered dark states. J. Am. Chem. Soc. 130 (50), 16840–16841.
[37] Vaughan, J.C., Dempsey, G.T., Sun, E. and Zhuang, X. (2013) Phosphine quenching of cyanine dyes as a versatile tool for fluorescence microscopy. J. Am. Chem. Soc. 135 (4), 1197–1200.
[38] Olivier, N., Keller, D., Gönczy, P. and Manley, S. (2013) Resolution doubling in 3D-STORM imaging through improved buffers. PLoS ONE 8 (7), e69004.
[39] Olivier, N., Keller, D., Rajan, V.S., Gönczy, P. and Manley, S. (2013) Simple buffers for 3D STORM microscopy. Biomed. Opt. Express. 4 (6), 885.
[40] Dickson, R.M., Cubitt, A.B., Tsien, R.Y. and Moerner, W.E. (1997) On/off blinking and switching behaviour of single molecules of green fluorescent protein. Nature 388 (6640), 355–358.
[41] Fernández-Suárez, M. and Ting, A.Y. (2008) Fluorescent probes for super-resolution imaging in living cells. Nat. Rev. Mol. Cell Biol. 9 (12), 929–943.
[42] Lippincott-Schwartz, J. and Patterson, G.H. (2009) Photoactivatable fluorescent proteins for diffraction-limited and super-resolution imaging. Trends Cell Biol. 19 (11), 555–565.
[43] Zhou, X.X. and Lin, M.Z. (2013) Photoswitchable fluorescent proteins: ten years of colorful chemistry and exciting applications. Curr. Opin. Chem. Biol. 17 (4), 682–690.
[44] Tiwari, D.K. and Nagai, T. (2013) Smart fluorescent proteins: innovation for barrier-free superresolution imaging in living cells. Dev. Growth Differ. 55 (4), 491–507.
[45] Dedecker, P., De Schryver, F.C. and Hofkens, J. (2013) Fluorescent proteins: shine on, you crazy diamond. J. Am. Chem. Soc. 135 (7), 2387–2402.

[46] Adam, V., Lelimousin, M., Boehme, S., Desfonds, G., Nienhaus, K., Field, M.J., et al. (2008) Structural characterization of IrisFP, an optical highlighter undergoing multiple photo-induced transformations. Proc. Natl. Acad. Sci. 105 (47), 18343–18348.

[47] Patterson, G.H. (2002) A photoactivatable GFP for selective photolabeling of proteins and cells. Science 297 (5588), 1873–1877.

[48] Ando, R. (2004) Regulated fast nucleocytoplasmic shuttling observed by reversible protein highlighting. Science 306 (5700), 1370–1373.

[49] Wiedenmann, J., Ivanchenko, S., Oswald, F., Schmitt, F., Röcker, C., Salih, A., et al. (2004) EosFP, a fluorescent marker protein with UV-inducible green-to-red fluorescence conversion. Proc. Natl. Acad. Sci. USA 101 (45), 15905–15910.

[50] Annibale, P., Scarselli, M., Kodiyan, A. and Radenovic, A. (2010) Photoactivatable fluorescent protein mEos2 displays repeated photoactivation after a long-lived dark state in the red photoconverted form. J. Phys. Chem. Lett. 1 (9), 1506–1510.

[51] Durisic, N., Laparra-Cuervo, L., Sandoval-Álvarez, Á., Borbely, J.S. and Lakadamyali, M. (2014) Single-molecule evaluation of fluorescent protein photoactivation efficiency using an in vivo nanotemplate. Nat. Methods 11 (2), 156–162.

[52] Müller, T., Schumann, C. and Kraegeloh, A. (2012) STED microscopy and its applications: new insights into cellular processes on the nanoscale. ChemPhysChem 13 (8), 1986–2000.

[53] Shaner, N.C., Lin, M.Z., McKeown, M.R., Steinbach, P.A., Hazelwood, K.L., Davidson, M.W., et al. (2008) Improving the photostability of bright monomeric orange and red fluorescent proteins. Nat. Methods 5 (6), 545–551.

[54] Willig, K.I., Kellner, R.R., Medda, R., Hein, B., Jakobs, S. and Hell, S.W. (2006) Nanoscale resolution in GFP-based microscopy. Nat. Methods 3 (9), 721–723.

[55] G. McNamara, PubSpectra – Open Data Access Fluorescence Spectra, <http://works.bepress.com/gmcnamara/9>.

[56] Nägerl, U.V., Willig, K.I., Hein, B., Hell, S.W. and Bonhoeffer, T. (2008) Live-cell imaging of dendritic spines by STED microscopy. Proc. Natl. Acad. Sci. 105 (48), 18982–18987.

[57] Griesbeck, O. (2001) Reducing the environmental sensitivity of yellow fluorescent protein. Mechanism and applications. J. Biol. Chem. 276 (31), 29188–29194.

[58] Hein, B., Willig, K.I. and Hell, S.W. (2008) Stimulated emission depletion (STED) nanoscopy of a fluorescent protein-labeled organelle inside a living cell. Proc. Natl. Acad. Sci. 105 (38), 14271–14276.

[59] Strack, R.L., Hein, B., Bhattacharyya, D., Hell, S.W., Keenan, R.J. and Glick, B.S. (2009) A rapidly maturing far-red derivative of dsred-express2 for whole-cell labeling. Biochemistry (Mosc) 48 (35), 8279–8281.

[60] Morozova, K.S., Piatkevich, K.D., Gould, T.J., Zhang, J., Bewersdorf, J. and Verkhusha, V.V. (2010) Far-red fluorescent protein excitable with red lasers for flow cytometry and superresolution STED nanoscopy. Biophys. J. 99 (2), L13–L15.

[61] Berning, S., Willig, K.I., Steffens, H., Dibaj, P. and Hell, S.W. (2012) Nanoscopy in a living mouse brain. Science 335 (6068), 551.

[62] Tønnesen, J., Nadrigny, F., Willig, K.I., Wedlich-Söldner, R. and Nägerl, U.V. (2011) Two-color STED microscopy of living synapses using a single laser-beam pair. Biophys. J. 101 (10), 2545–2552.

[63] Grotjohann, T., Testa, I., Leutenegger, M., Bock, H., Urban, N.T., Lavoie-Cardinal, F., et al. (2011) Diffraction-unlimited all-optical imaging and writing with a photochromic GFP. Nature 478 (7368), 204–208.

[64] Brakemann, T., Stiel, A.C., Weber, G., Andresen, M., Testa, I., Grotjohann, T., et al. (2011) A reversibly photoswitchable GFP-like protein with fluorescence excitation decoupled from switching. Nat. Biotechnol. 29 (10), 942–947.

[65] Grotjohann, T., Testa, I., Reuss, M., Brakemann, T., Eggeling, C., Hell, S.W., et al. (2012) RsEGFP2 enables fast RESOLFT nanoscopy of living cells. Elife 1 (1), 1–14.

[66] Lavoie-Cardinal, F., Jensen, N.A., Westphal, V., Stiel, A.C., Chmyrov, A., Bierwagen, J., et al. (2014) Two-color RESOLFT nanoscopy with green and red fluorescent photochromic proteins. ChemPhysChem 21 (15), 655–663.

[67] McKinney, S.A., Murphy, C.S., Hazelwood, K.L., Davidson, M.W. and Looger, L.L. (2009) A bright and photostable photoconvertible fluorescent protein. Nat. Methods 6 (2), 131–133.

[68] Jones, S.A., Shim, S.-H., He, J. and Zhuang, X. (2011) Fast, three-dimensional super-resolution imaging of live cells. Nat. Methods 8 (6), 499–505.

[69] McEvoy, A.L., Hoi, H., Bates, M., Platonova, E., Cranfill, P.J., Baird, M.A., et al. (2012) MMaple: a photoconvertible fluorescent protein for use in multiple imaging modalities. PLoS ONE 7 (12), e51314.

[70] Zhang, M., Chang, H., Zhang, Y., Yu, J., Wu, L., Ji, W., et al. (2012) Rational design of true monomeric and bright photoactivatable fluorescent proteins. Nat. Methods 9 (7), 727–729.

[71] Habuchi, S., Ando, R., Dedecker, P., Verheijen, W., Mizuno, H., Miyawaki, A., et al. (2005) Reversible single-molecule photoswitching in the GFP-like fluorescent protein Dronpa. Proc. Natl. Acad. Sci. USA 102 (27), 9511–9516.

[72] Moeyaert, B., Nguyen Bich, N., De Zitter, E., Rocha, S., Clays, K., Mizuno, H., et al. (2014) Green-to-red photoconvertible dronpa mutant for multimodal super-resolution fluorescence microscopy. ACS Nano 8 (2), 1664–1673.

[73] Jensen, N.A., Danzl, J.G., Willig, K.I., Lavoie-Cardinal, F., Brakemann, T., Hell, S.W., et al. (2014) Coordinate-targeted and coordinate-stochastic super-resolution microscopy with the reversibly switchable fluorescent protein dreiklang. ChemPhysChem. n/a–n/a.

[74] Nie, S., Chiu, D.T. and Zare, R.N. (1994) Probing individual molecules with confocal fluorescence microscopy. Science 266 (5187), 1018–1021.

[75] Basche, T., Kummer, S. and Brauchle, C. (1995) Direct spectroscopic observation of quantum jumps of a single molecule. Nature 373 (6510), 132–134.

[76] Bates, M., Blosser, T. and Zhuang, X. (2005) Short-range spectroscopic ruler based on a single-molecule optical switch. Phys. Rev. Lett. 94 (10), http://dx.doi.org/10.1103/PhysRevLett. 94.108101.

[77] Heilemann, M., Margeat, E., Kasper, R., Sauer, M. and Tinnefeld, P. (2005) Carbocyanine dyes as efficient reversible single-molecule optical switch. J. Am. Chem. Soc. 127 (11), 3801–3806.

[78] Bates, M., Huang, B., Dempsey, G.T. and Zhuang, X. (2007) Multicolor super-resolution imaging with photo-switchable fluorescent probes. Science 317 (5845), 1749.

[79] Fölling, J., Bossi, M., Bock, H., Medda, R., Wurm, C.A., Hein, B., et al. (2008) Fluorescence nanoscopy by ground-state depletion and single-molecule return. Nat. Methods 5 (11), 943–945.

[80] Heilemann, M., van de Linde, S., Mukherjee, A. and Sauer, M. (2009) Super-resolution imaging with small organic fluorophores. Angew. Chem. Int. Ed. 48 (37), 6903–6908.

[81] Kolmakov, K., Wurm, C.A., Meineke, D.N.H., Göttfert, F., Boyarskiy, V.P., Belov, V.N., et al. (2014) Polar red-emitting rhodamine dyes with reactive groups: synthesis, photophysical properties, and two-color STED nanoscopy applications. Chem. Eur. J. 20 (1), 146–157.

[82] Abberior, <http://www.abberior.com/home/>.

[83] Meyer, L., Wildanger, D., Medda, R., Punge, A., Rizzoli, S.O., Donnert, G., et al. (2008) Dual-color STED microscopy at 30-nm focal-plane resolution. Small 4 (8), 1095–1100.

[84] Testa, I., Wurm, C.A., Medda, R., Rothermel, E., von Middendorf, C., Fölling, J., et al. (2010) Multicolor fluorescence nanoscopy in fixed and living cells by exciting conventional fluorophores with a single wavelength. Biophys. J. 99 (8), 2686–2694.

[85] Ries, J., Kaplan, C., Platonova, E., Eghlidi, H. and Ewers, H. (2012) A simple, versatile method for GFP-based super-resolution microscopy via nanobodies. Nat. Methods 9 (6), 582–584.

[86] Shim, S.H., Xia, C., Zhong, G., Babcock, H.P., Vaughan, J.C., Huang, B., et al. (2012) Super-resolution fluorescence imaging of organelles in live cells with photoswitchable membrane probes. Proc. Natl. Acad. Sci. 109 (35), 13978–13983.

[87] Lukinavičius, G., Reymond, L., D'Este, E., Masharina, A., Göttfert, F., Ta, H., et al. (2014) Fluorogenic probes for live-cell imaging of the cytoskeleton. Nat. Methods. Available from: http://www.nature.com/doifinder/10.1038/nmeth.2972.

[88] Hinner, M.J. and Johnsson, K. (2010) How to obtain labeled proteins and what to do with them. Curr. Opin. Biotechnol. 21 (6), 766–776.

[89] Jing, C. and Cornish, V.W. (2011) Chemical tags for labeling proteins inside living cells. Acc. Chem. Res. 44 (9), 784–792.

[90] Chen, Z., Cornish, V.W. and Min, W. (2013) Chemical tags: inspiration for advanced imaging techniques. Curr. Opin. Chem. Biol. 17 (4), 637–643.

[91] Dempsey, G.T., Bates, M., Kowtoniuk, W.E., Liu, D.R., Tsien, R.Y. and Zhuang, X. (2009) Photoswitching mechanism of cyanine dyes. J. Am. Chem. Soc. 131 (51), 18192–18193.

[92] Van de Linde, S., Krstić, I., Prisner, T., Doose, S., Heilemann, M. and Sauer, M. (2010) Photoinduced formation of reversible dye radicals and their impact on super-resolution imaging. Photochem. Photobiol. Sci. 15 (10), 499–506.

[93] Kottke, T., van de Linde, S., Sauer, M., Kakorin, S. and Heilemann, M. (2010) Identification of the product of photoswitching of an oxazine fluorophore using fourier transform infrared difference spectroscopy. J. Phys. Chem. Lett. 1, 3156–3159.

[94] Lord, S.J., Conley, N.R., Lee, H.D., Samuel, R., Liu, N., Twieg, R.J., et al. (2008) A photoactivatable Push-Pull fluorophore for single-molecule imaging in live cells. J. Am. Chem. Soc. 130 (29), 9204–9205.

[95] Lord, S., Lee, H., Samuel, R., Weber, R., Liu, N., Conley, N., et al. (2010) Azido push-pull fluorogens photoactivate to produce bright fluorescent labels. J. Phys. Chem. B 114 (45), 14157–14167.

[96] Belov, V.N., Wurm, C.A., Boyarskiy, V.P., Jakobs, S. and Hell, S.W. (2010) Rhodamines NN: a novel class of caged fluorescent dyes. Angew. Chem. Int. Ed. 49 (20), 3520–3523.

[97] Wysocki, L.M., Grimm, J.B., Tkachuk, A.N., Brown, T.A., Betzig, E. and Lavis, L.D. (2011) Facile and general synthesis of photoactivatable xanthene dyes. Angew. Chem. Int. Ed. 50 (47), 11206–11209.

[98] Grimm, J.B., Sung, A.J., Legant, W.R., Hulamm, P., Matlosz, S.M., Betzig, E., et al. (2013) Carbofluoresceins and carborhodamines as scaffolds for high-contrast fluorogenic probes. ACS Chem. Biol. 8 (6), 1303–1310.

[99] Mitronova, G.Y., Belov, V.N., Bossi, M.L., Wurm, C.A., Meyer, L., Medda, R., et al. (2010) New fluorinated rhodamines for optical microscopy and nanoscopy. Chem. Eur. J. 16 (15), 4477–4488.

[100] Kolmakov, K., Wurm, C.A., Hennig, R., Rapp, E., Jakobs, S., Belov, V.N., et al. (2012) Red-emitting rhodamines with hydroxylated, sulfonated, and phosphorylated dye residues and their use in fluorescence nanoscopy. Chem. Eur. J. 18 (41), 12986–12998.

[101] Göttfert, F., Wurm, C.A., Mueller, V., Berning, S., Cordes, V.C., Honigmann, A., et al. (2013) Coaligned dual-channel sted nanoscopy and molecular diffusion analysis at 20 nm resolution. Biophys. J. 105 (1), L01–L03.

[102] Belov, V.N. and Bossi, M.L. (2013) Photoswitching emission with rhodamine spiroamides for super-resolution fluorescence nanoscopies. Isr. J. Chem. 53 (5), 267–279.

[103] Rasnik, I., McKinney, S.A. and Ha, T. (2006) Nonblinking and long-lasting single-molecule fluorescence imaging. Nat. Methods 3 (11), 891–893.
[104] Vogelsang, J., Kasper, R., Steinhauer, C., Person, B., Heilemann, M., Sauer, M., et al. (2008) A reducing and oxidizing system minimizes photobleaching and blinking of fluorescent dyes. Angew. Chem. Int. Ed. 47 (29), 5465–5469.
[105] Fölling, J., Belov, V., Kunetsky, R., Medda, R., Schönle, A., Egner, A., et al. (2007) Photochromic rhodamines provide nanoscopy with optical sectioning. Angew. Chem. Int. Ed. 46 (33), 6266–6270.
[106] Lord, S.J., Conley, N.R., Lee, H.D., Nishimura, S.Y., Pomerantz, A.K., Willets, K.A., et al. (2009) DCDHF fluorophores for single-molecule imaging in cells. ChemPhysChem 10 (1), 55–65.
[107] Ha, T. and Tinnefeld, P. (2012) Photophysics of fluorescent probes for single-molecule biophysics and super-resolution imaging. Annu. Rev. Phys. Chem. 63 (1), 595–617.
[108] Schäfer, P., van de Linde, S., Lehmann, J., Sauer, M. and Doose, S. (2013) Methylene blue- and thiol-based oxygen depletion for super-resolution imaging. Anal. Chem. 85 (6), 3393–3400.
[109] Lee, S.F., Vérolet, Q. and Fürstenberg, A. (2013) Improved super-resolution microscopy with oxazine fluorophores in heavy water. Angew. Chem. Int. Ed. 52 (34), 8948–8951.
[110] Klehs, K., Spahn, C., Endesfelder, U., Lee, S.F., Fürstenberg, A. and Heilemann, M. (2013) Increasing the brightness of cyanine fluorophores for single-molecule and superresolution imaging. ChemPhysChem 2 (15), 637–641.
[111] Active Motif, <http://www.activemotif.com/catalog/69/fluorescent-dyes-and-antibodies>.
[112] Pellett, P.A., Sun, X., Gould, T.J., Rothman, J.E., Xu, M.-Q., Corrêa, I.R., et al. (2011) Two-color STED microscopy in living cells. Biomed. Opt. Express 2 (8), 2364–2371.
[113] Bingen, P., Reuss, M., Engelhardt, J. and Hell, S.W. (2011) Parallelized STED fluorescence nanoscopy. Opt. Express 19 (24), 23716–23726.
[114] Willig, K.I., Harke, B., Medda, R. and Hell, S.W. (2007) STED microscopy with continuous wave beams. Nat. Methods 4 (11), 915–918.
[115] ATTO-TEC, <https://www.atto-tec.com/>.
[116] Wurm, C.A., Kolmakov, K., Göttfert, F., Ta, H., Bossi, M., Schill, H., et al. (2012) Novel red fluorophores with superior performance in STED microscopy. Opt. Nanoscopy 1 (1), 1–7.
[117] Lukinavičius, G., Umezawa, K., Olivier, N., Honigmann, A., Yang, G., Plass, T., et al. (2013) A near-infrared fluorophore for live-cell super-resolution microscopy of cellular proteins. Nat. Chem. 5 (2), 132–139.
[118] GE Healthcare, <http://www.gelifesciences.com/webapp/wcs/stores/servlet/catalog/en/GELifeSciences/brands/cydye/>.
[119] Molecular Probes, <http://www.lifetechnologies.com/us/en/home/brands/molecular-probes.html>.
[120] Dertinger, T., Colyer, R., Iyer, G., Weiss, S. and Enderlein, J. (2009) Fast, background-free, 3D super-resolution optical fluctuation imaging (SOFI). Proc. Natl. Acad. Sci. 106 (52), 22287–22292.
[121] Cox, S., Rosten, E., Monypenny, J., Jovanovic-Talisman, T., Burnette, D.T., Lippincott-Schwartz, J., et al. (2011) Bayesian localization microscopy reveals nanoscale podosome dynamics. Nat. Methods 9 (2), 195–200.
[122] Lidke, K.A., Rieger, B., Jovin, T.M. and Heintzmann, R. (2005) Superresolution by localization of quantum dots using blinking statistics. Opt. Express 13 (18), 7052–7062.
[123] Irvine, S.E., Staudt, T., Rittweger, E., Engelhardt, J. and Hell, S.W. (2008) Direct light-driven modulation of luminescence from Mn-doped ZnSe quantum dots. Angew. Chem. Int. Ed. 47 (14), 2685–2688.
[124] Hoyer, P., Staudt, T., Engelhardt, J. and Hell, S.W. (2011) Quantum dot blueing and blinking enables fluorescence nanoscopy. Nano Lett., 413–468.
[125] Howarth, M., Liu, W., Puthenveetil, S., Zheng, Y., Marshall, L.F., Schmidt, M.M., et al. (2008) Monovalent, reduced-size quantum dots for imaging receptors on living cells. Nat. Methods 5 (5), 397–399.
[126] Sharonov, A. and Hochstrasser, R.M. (2006) Wide-field subdiffraction imaging by accumulated binding of diffusing probes. Proc. Natl. Acad. Sci. 103 (50), 18911.
[127] Jungmann, R., Steinhauer, C., Scheible, M., Kuzyk, A., Tinnefeld, P. and Simmel, F.C. (2010) Single-molecule kinetics and super-resolution microscopy by fluorescence imaging of transient binding on DNA origami. Nano Lett. 10 (11), 4756–4761.
[128] Jungmann, R., Avendaño, M.S., Woehrstein, J.B., Dai, M., Shih, W.M. and Yin, P. (2014) Multiplexed 3D cellular super-resolution imaging with DNA-PAINT and Exchange-PAINT. Nat. Methods 11 (3), 313–318.